CrossMark

Highly luminescent, high-indium-content InGaN film with uniform composition and full misfit-strain relaxation

A. M. Fischer,[1] Y. O. Wei,[1] F. A. Ponce,[1,a)] M. Moseley,[2] B. Gunning,[2] and W. A. Doolittle[2]
[1]*Department of Physics, Arizona State University, Tempe, Arizona 85287-1504, USA*
[2]*Advanced Semiconductor Technology Facility, School of Electrical and Computer Engineering, Georgia Institute of Technology, Atlanta, Georgia 30332, USA*

(Received 6 February 2013; accepted 9 September 2013; published online 24 September 2013)

We have studied the properties of thick $In_xGa_{1-x}N$ films, with indium content ranging from $x \sim 0.22$ to 0.67, grown by metal-modulated epitaxy. While the low indium-content films exhibit high density of stacking faults and dislocations, a significant improvement in the crystalline quality and optical properties has been observed starting at $x \sim 0.6$. Surprisingly, the $In_xGa_{1-x}N$ film with $x \sim 0.67$ exhibits high luminescence intensity, low defect density, and uniform full lattice-mismatch strain relaxation. The efficient strain relaxation is shown to be due to a critical thickness close to the monolayer range. These films were grown at low temperatures (∼400 °C) to facilitate indium incorporation and with precursor modulation to enhance surface morphology and metal adlayer diffusion. These findings should contribute to the development of growth techniques for nitride semiconductors under high lattice misfit conditions. © *2013 AIP Publishing LLC*.
[http://dx.doi.org/10.1063/1.4822122]

InGaN films with high indium content are necessary for the development of green and longer wavelength optoelectronic devices and of high-efficiency photovoltaic solar cells. An important limitation is indium incorporation during growth, requiring low temperatures at the expense of nitrogen compound dissociation.[1] In addition, the absence of bulk InGaN crystals limits InGaN growth to substrates with substantial difference in lattice parameter, such as GaN layers deposited on sapphire or SiC. The lattice mismatch can be as large as ∼10.6% in the case of InN on GaN. Lattice-mismatch strain relaxation in InGaN/GaN layers has been observed to occur in various ways although not necessarily improving the crystalline quality of the film.[2,3] In *c*-plane epitaxy, misfit dislocations may be introduced by glide along the basal plane,[4] by glide along the $\{11\bar{2}2\}\langle 11\bar{2}3\rangle$ slip system,[3] and by bending of dislocations threading from the GaN underlayer.[5] Growth of InGaN films is also affected by compositional instabilities, with predicted spinodal decomposition over a wide range of indium content.[6,7] However, $In_xGa_{1-x}N$ films with $x \leq 0.25$ have been reported to grow without phase separation by molecular beam epitaxy (MBE) in the growth temperature range of 650–675 °C.[8] It has also been shown that uniform InGaN layers can be grown at lower temperatures without phase separation over a wide range of indium compositions using metal-modulated epitaxy,[9] a modified MBE technique where the metal flux is periodically modulated to enhance surface adlayer diffusion while the nitrogen flux is kept constant.

In this letter, we report on the optical and structural properties of thick $In_xGa_{1-x}N$ films grown by the metal-modulated epitaxy technique, with indium content ranging from $x = 0.22$ to 0.67. At $x \sim 0.60$, we observe a significant improvement in the crystalline structure of the $In_xGa_{1-x}N$ films. This transition is from layers with high densities of crystal defects to layers that are defect free and exhibit full and uniform misfit strain relaxation at the InGaN/GaN interface. In particular, layers with $x = 0.67$ exhibit a surprisingly strong photoluminescence (PL) peak at 1300 nm, compared to films with lower indium content.

The $In_xGa_{1-x}N$ films were grown on GaN epilayers on sapphire, at temperatures between 400 and 450 °C, with a total group-III beam equivalent pressure of 0.24×10^{-7} Torr. The open time of the metal shutter was optimized to achieve indium compositions of $x = 0.22$, 0.46, 0.6, and 0.67. The thin-film structure was capped with a 10-nm-thick GaN layer to prevent thermal decomposition during the cool-down period that follows growth.[10] More detail about the growth conditions can be found elsewhere.[11] The indium composition in the InGaN layers was measured by standard x-ray diffraction (XRD) analysis. To confirm the XRD measurements, we have used Rutherford backscattered spectroscopy (RBS). Fig. 1 shows the spectrum for the film with the highest indium composition. The data were obtained in a General Ionex 1.7 MV high current tandem accelerator (Tandetron) using a He^{++} beam with an energy of 2 MeV. The fitted curve, simulated using a standard RBS analysis package,[12] indicates that the indium content in this layer is $x = 0.67 \pm 0.01$, in close agreement with the XRD measurement.

Figure 2 shows cross-section transmission electron microscopy (TEM) images of the microstructure of the InGaN films, observed along a $\langle 11\bar{2}0\rangle$ projection with $\boldsymbol{g} = [1\bar{1}00]$. The cross-section samples were prepared by standard polishing followed by argon ion milling. The microstructure was analyzed in a JEOL 4000-EX TEM operated at 400 kV. The thickness of the InGaN films was determined from the TEM images to be ∼50 nm. The images in Fig. 2 illustrate the evolution of the microstructure under increasing lattice mismatch. Fig. 2(a) shows that for $x = 0.22$ incoherent plastic relaxation leads to the formation of a large density of basal-

[a)]Author to whom correspondence should be addressed. Electronic mail: ponce@asu.edu

 © 2013 AIP Publishing LLC

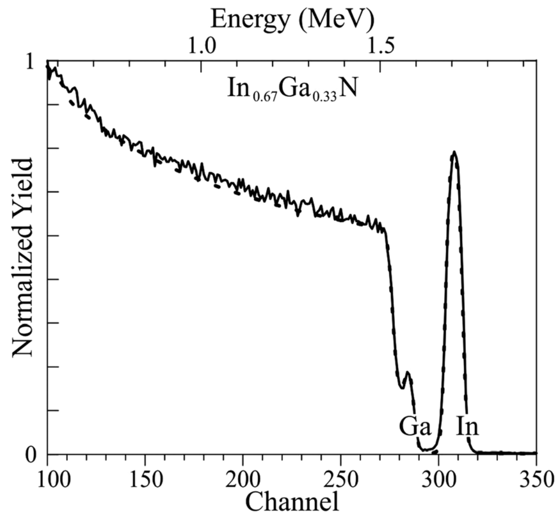

FIG. 1. Rutherford backscattered spectrum of the InGaN film with the highest indium content, which is found to be $x = 0.67 \pm 0.01$. Dotted line represents the fitting with RUMP simulation.

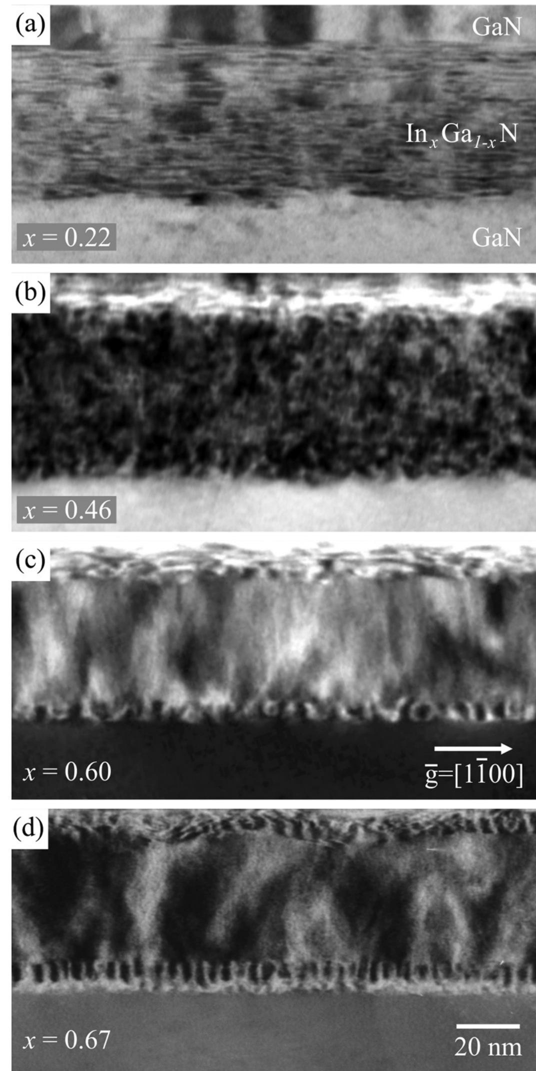

FIG. 2. Cross-section TEM images of the InGaN films, taken along the $\langle 11\bar{2}0\rangle$ projection with diffraction contrast set at $\boldsymbol{g} = [1\bar{1}00]$. High density of basal plane stacking faults and dislocations are observed for (a) $x = 0.22$ and (b) $x = 0.46$. Misfit strain relaxation is observed as moiré fringes at the InGaN/GaN interfaces for (c) $x = 0.60$ and (d) $x = 0.67$.

plane stacking faults with dimensions of ~20 nm. Increasing the indium composition to $x = 0.46$ (see Fig. 2(b)) results in a granular structure with dimensions of the order of 10 nm; stacking faults are not easily observed in this case. The characteristics of the $In_xGa_{1-x}N$ film do change significantly for $x = 0.60$ in Fig. 2(c), where the film shows improved uniformity, with no stacking faults or grain boundaries present. At this composition, moiré fringes are observed at the InGaN/GaN lower and upper heterojunctions, indicating full strain relaxation at the interfaces by the generation of misfit dislocations. In fact, from geometric considerations the separation of the moiré fringes is the same as the distance between misfit dislocations. The microstructure is further improved for $x = 0.67$ in Fig. 2(d), where a uniform array of moiré fringes is observed. The distance D between the fringes (~4.06 ± 0.04 nm in the bottom interface) is due to the difference in interplanar separation across the InGaN/GaN interface

$$D = \frac{d_{InGaN} \cdot d_{GaN}}{d_{InGaN} - d_{GaN}}, \qquad (1)$$

where d_{GaN} and d_{InGaN} are the interplanar distances in the GaN and InGaN layers. The moiré fringes are arranged along $\langle 11\bar{2}0\rangle$ directions, where the interplanar separation is $d = a\frac{\sqrt{3}}{2}$ (a is the lattice parameter in the basal plane). Using Eq. (1), we get $\Delta a = a_{InGaN} - a_{GaN} = 0.0232 \pm 0.002$ nm. This corresponds to an indium content in the $In_xGa_{1-x}N$ layer of $x = 0.66 \pm 0.05$, in agreement with the RBS spectrum in Fig. 1. Similar results were obtained by direct measurement of the difference in lattice parameter from high-resolution TEM images of the InGaN/GaN interface region (not shown here). Thus, the moiré fringe separation and the high-resolution TEM images indicate complete lattice misfit strain relaxation at the InGaN/GaN interface.

TEM images of the $In_{0.67}Ga_{0.33}N$ film taken with $g = [11\bar{2}0]$, not shown here, exhibit alternating bright and dark regions indicating a columnar structure with low-angle grain boundaries associated with slight crystal rotations about the c-axis.[13] It should be noted that the columnar width and the layer thickness values are of the order of 50 nm. Undulations at the top surface were observed along the $\langle 1\bar{1}00\rangle$ and $\langle 11\bar{2}0\rangle$ projections, the latter one shown in Fig. 2(d), implying the presence of a cross-hatch surface morphology, with hillocks separated by ~45 nm along the $\langle 11\bar{2}0\rangle$ directions. This is consistent with the presence of the low-angle domain boundaries discussed before.

Figure 3 shows XRD rocking curves of the (002) GaN and (002) $In_{0.67}Ga_{0.33}N$ diffraction peaks. The GaN curve in Fig. 3(a) has been fitted with two Gaussian curves. Based on the diffraction intensities, we assign these curves to the GaN underlayer and to the GaN capping layer. The full-width-at-half-maximum (FWHM) of the GaN underlayer is ~5.8 arc min whereas of the GaN capping layer is ~11.6 arc min. The latter has a larger FWHM due to growth on the InGaN layer with a FWHM of ~8.5 arc min in Fig. 3(b).

The optical properties of the films were studied by photoluminescence spectroscopy. The films were cooled to a temperature of 10 K. A double-frequency Nd:YAG (532 nm) laser with a power of 5 mW was used for excitation. The spectrum was generated using a 600 lines/mm grating, and

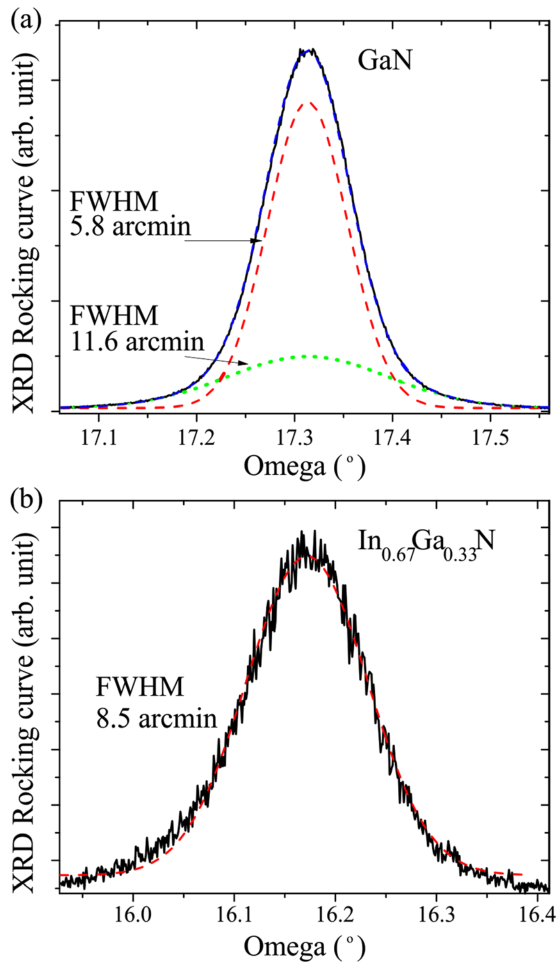

FIG. 3. X-ray rocking curves of (a) the GaN underlayer (FWHM = 5.8 arc min) and capping layer (FWHM = 11.6 arc min) and (b) the $In_{0.67}Ga_{0.33}N$ film (FWHM = 8.5 arc min). Dashed lines represent Gaussian fits.

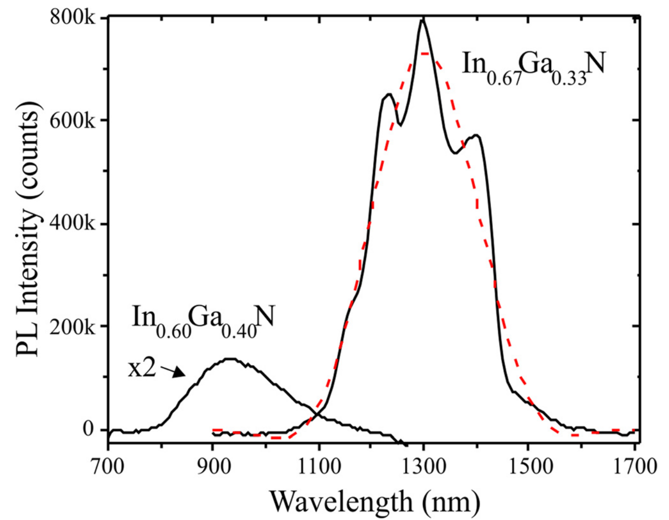

FIG. 4. Photoluminescence spectra of the InGaN films with $x = 0.6$ and 0.67, taken at a temperature of 10 K. The dashed line has been obtained by removing the interference produced by the 4-μm-thick GaN underlayer.

the light intensity was measured with a Ge photodiode with an integration time of one second. Negligible luminescence was observed for $In_xGa_{1-x}N$ films with $0.22 \leq x < 0.60$ (not shown here). The onset of luminescence was observed at $x = 0.60$. Fig. 4 shows the luminescence corresponding to the films with $x = 0.60$ and 0.67. The former exhibits a peak centered at $\sim$930 nm with an emission intensity of approximately one order of magnitude lower than the latter. The dominant peak for $x = 0.67$ is centered at $\sim$1300 nm, and it is modulated by Fabry-Pérot interference. The thickness of the layer that produces the Fabry-Pérot interference peak maxima (at $\lambda_1 = 1169$, $\lambda_2 = 1225$, and $\lambda_3 = 1399$ nm in Fig. 4) can be calculated using Bragg's law by plotting $2\,n(\lambda_m)/\lambda_m$ vs. m, where $n(\lambda_m)$ is the index of refraction for the peak wavelengths; the index of refraction can be found for GaN using the Sellmeier equation.[14,15] In this manner, the interfering layer thickness is found to be $\sim 4\,\mu$m, which matches well with the GaN underlayer thickness measured by TEM. By removing the interference effects (dashed line in Fig. 4), the $In_{0.67}Ga_{0.33}N$ emission wavelength is found to be 1300 nm with a FWHM of 236 nm.

The crystalline and optical quality of the $In_{0.67}Ga_{0.33}N$ film is reflected in the XRD and PL spectra. The θ-2θ XRD peak linewidth (not shown here) for this film is 9.9 arc min, and its value can be explained in terms of the crystal domain size using the Scherrer equation, $d = K\lambda/\beta\cos\theta$,[16] with the Scherrer constant $K = 0.88$ (for cubic-shaped crystallites),[17] the wavelength for the K_α line of copper $\lambda = 0.15406$ nm, the Bragg angle $\theta = 16.13°$, and $\beta = 9.89$ arc min is the square root of the difference of the squares of the measured linewidth (9.9 arc min), and the instrumental linewidth broadening (0.2 arc min). The Scherrer equation gives a particle size $d = 49$ nm, which is close to the film thickness and crystal domain dimensions of $\sim$50 nm in our materials. For the optical properties, the observed low-temperature PL linewidth of 175 meV (236 nm) can be explained by taking into consideration alloy broadening effects associated with statistical fluctuation of indium and gallium at cation sites.[18] Alloy broadening in $In_xGa_{1-x}N$ alloys have been reported to be $\sim$155 meV for an indium content of $x \approx 0.67$.[19] Thus, the linewidth broadening of the XRD and PL spectra is due to particle size and uniform random alloy distribution, respectively. It is not due to crystal defects or large-scale compositional fluctuations. We may therefore conclude that our material is of high quality from the optical and structural points of view.

Epilayers with lower indium content ($x < 0.60$), grown under similar conditions, did not exhibit significant luminescent characteristics due to their inferior structural properties which should be associated with a high density of nonradiative centers that reduce the emission efficiency. The transition from poor to high quality InGaN films can be explained by lattice-mismatch strain relaxation at the InGaN/GaN interface via the generation of misfit dislocations after a critical thickness is achieved. Early critical thickness models consider that misfit dislocation generation occurs when the force due to the misfit stress is equal to the dislocation line tension (force balance model).[20,21] In our case, the Peierls' force should also be taken into account since the growth temperature and the threading dislocation density are low.[22] Our observations are consistent with theoretical calculations of the critical thickness for dislocation generation for epitaxy of InGaN on (0001) GaN (see Fig. 5).[20–24] Due to the nature of the transcendental equations, these calculations are only feasible up to $x \approx 0.40$. In Fig. 5 we extrapolate the curves to

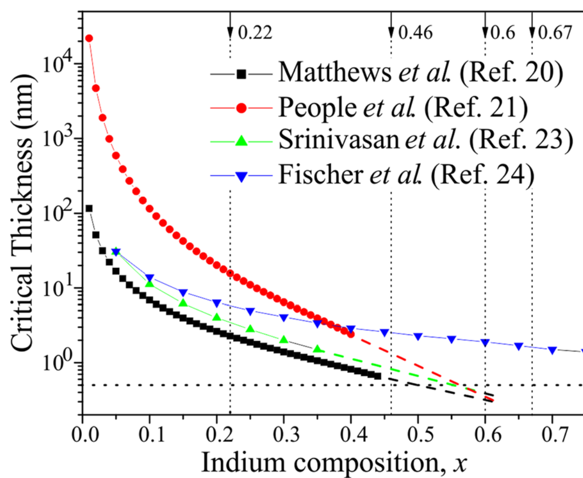

FIG. 5. Critical thickness vs. indium content x for the $In_xGa_{1-x}N$/GaN system using various models.[20–24] The critical thickness of one lattice period c (horizontal dotted line) happens at $x \sim 0.55$.

values of the critical thickness of about one lattice parameter. In the case of Fischer's model,[24] the critical thickness of the film is determined using bulk material behavior—this being the reason for the larger values of the critical thickness for $x > 0.4$. We envision that under large lattice mismatch, the material is unstable until a sufficient number of atoms are available for the material to acquire its own identity, at which point it crystallizes with its own lattice parameter, and misfit dislocations appear spontaneously. This should happen when the critical thickness for plastic deformation is of the order of a few monolayers. For such thin films, considerations of dislocation glide on the crystal planes are not necessary. The subsequent growth then happens under relaxed conditions leading to a low defect density and high luminescent properties. We propose that the metal-modulated epitaxy technique contributes to the planarity of growth and to the uniformity in lattice-misfit strain relaxation.

In summary, we report an unexpected and substantial improvement in the properties of InGaN films with high indium content. InGaN epilayers grown on GaN by metal-modulated epitaxy at low temperatures exhibit a transition in the structural properties at $x = 0.60$. X-ray diffraction shows that the structural properties are of high quality, with the diffraction peak widths fully explained by particle size broadening. Photoluminescence spectroscopy also shows material of high quality, with the luminescence peak being fully explained by alloy disordering considerations. Critical thickness calculations using various models show that observed transitions coincide with the critical thickness reaching a value in the range of the crystal lattice parameter. We propose that for critical thicknesses close to a monolayer the material spontaneously nucleates in a *fully relaxed* state, with a periodic network of misfit dislocations. This happens at uniform layer growth conditions. Growth of high indium content films with superior optical properties due to uniform misfit strain relaxation should enable the development of longer-wavelength devices for applications in solid-state lighting and photovoltaics.

This material was based upon work supported in part by the National Science Foundation (NSF) and the Department of Energy (DOE) under NSF CA No. EEC-1041895 and in part by the NSF Materials World Network under grant NSF CA No. DMR-1108450.

[1] I. Akasaki and H. Amano, J. Cryst. Growth **146**, 455 (1995).
[2] H. K. Cho, J. Y. Lee, J. H. Song, P. W. Yu, G. M. Yang, and C. S. Kim, J. Appl. Phys. **91**, 1104 (2002).
[3] R. Liu, J. Mei, S. Srinivasan, H. Omiya, F. A. Ponce, D. Cherns, Y. Narukawa, and T. Mukai, Jpn. J. Appl. Phys. **45**, L549 (2006).
[4] R. Liu, J. Mei, S. Srinivasan, F. A. Ponce, H. Omiya, Y. Narukawa, and T. Mukai, Appl. Phys. Lett. **89**, 201911 (2006).
[5] Z. H. Wu, K. Nonaka, Y. Kawai, T. Asai, F. A. Ponce, C. Q. Chen, M. Iwaya, S. Kamiyama, H. Amano, and I. Akasaki, Appl. Phys. Express **3**, 111003 (2010).
[6] F. A. Ponce, S. Srinivasan, A. Bell, L. Geng, R. Liu, M. Stevens, J. Cai, H. Omiya, H. Marui, and S. Tanaka, Phys. Status Solidi A **240**, 273 (2003).
[7] I. Ho and G. B. Stringfellow, Appl. Phys. Lett. **69**, 2701 (1996).
[8] D. Doppalapudi, S. N. Basu, K. F. Ludwig, Jr., and T. D. Moustakas, J. Appl. Phys. **84**, 1389 (1998).
[9] M. Moseley, J. Lowder, D. Billingsley, and W. A. Doolittle, Appl. Phys. Lett. **97**, 191902 (2010).
[10] R. Singh, D. Doppalapudi, T. D. Moustakas, and L. T. Romano, Appl. Phys. Lett. **70**, 1089 (1997).
[11] M. Moseley, B. Gunning, J. Greenlee, J. Lowder, G. Namkoong, and W. A. Doolittle, J. Appl. Phys. **112**, 014909 (2012).
[12] RUMP, Program for the simulation and analysis of RBS data. See: W. K. Chu, J. W. Mayer, and M.-A. Nicolet, *Backscattering Spectrometry* (Academic Press, NY, 1978); and L. R. Doolittle, Nucl. Inst. Meth. B **9**, 344 (1985).
[13] F. A. Ponce, MRS Bull. **22**, 51 (1997).
[14] W. Sellmeier, Ann. Phys. Chem. **219**, 272 (1871).
[15] A. S. Barker, Jr. and M. Ilegems, Phys. Rev. B **7**, 743 (1973).
[16] P. Scherrer, Göttinger Nachrichten Math. Phys. **2**, 98 (1918).
[17] J. I. Langford and A. J. C. Wilson, J. Appl. Cryst. **11**, 102 (1978).
[18] E. F. Schubert, E. O. Göbel, Y. Horikoshi, K. Ploog, and H. J. Queisser, Phys. Rev. B **30**, 813 (1984).
[19] T. Suski, G. Franssen, A. Kamińska, A. Khachapuridze, H. Teisseyre, J. A. Plesiewicz, L. H. Dmowski, H. Lu, W. J. Schaff, M. Kurouchi, and Y. Nanishi, Proc. SPIE **6473**, 647311 (2007).
[20] J. W. Matthews and A. E. Blakeslee, J. Cryst. Growth **27**, 118 (1974).
[21] R. People and J. C. Bean, Appl. Phys. Lett. **47**, 322 (1985).
[22] J. W. Matthews, S. Mader, and T. B. Light, J. Appl. Phys. **41**, 3800 (1970).
[23] S. Srinivasan, L. Geng, R. Liu, F. A. Ponce, Y. Narukawa, and S. Tanaka, Appl. Phys. Lett. **83**, 5187 (2003).
[24] A. Fischer, H. Kühne, and H. Richter, Phys. Rev. Lett. **73**, 2712 (1994).